

# An Efficient Multipaction Analysis of an Output Multiplexer for Satellite Applications

Man Seok Uhm<sup>1</sup> · Juseop Lee<sup>2</sup> · In-Bok Yom<sup>1</sup> · Jeong-Phill Kim<sup>3</sup>

## Abstract

In this paper, an efficient multipaction analysis method of a manifold multiplexer for satellite applications is presented. While FEM(Finite Element Method) is used for the multipaction analysis of the lowpass filter, the equivalent circuit model is used for the analysis of the channel filters and the manifold. Employing equivalent circuit model for multipaction analysis takes less time than using EM(Electromagnetic) field analysis method while keeping the accuracy of the multipaction analysis. This present analysis method is applied to the manifold multiplexer for Ka-band satellite transponders and the results show that the present method is as accurate as the conventional EM field analysis method.

**Key words** : Multiplexer, OMUX, Channel Filter, Manifold, Dual-mode Filter, Multipaction.

## I. Introduction

In communication systems, the available frequency spectrum is a primary resource. The channelization of the frequency band into a number of RF channels is required due to the practical constraints of non-linearity in the high power amplifiers<sup>[1]</sup>. The multiplexing equipment for satellite applications requires the lowest insertion loss to obtain the optimal efficiency with the limited dc power and the lowest mass due to the high launch cost of the payload. The manifold multiplexing technique provides the lowest insertion losses as well as the most compact size and the minimum mass in contrast to the other multiplexing methods. Therefore, the manifold multiplexing technique is largely applied to the output multiplexer(OMUX) for satellite transponders.

Many design methods for the manifold multiplexer have been reported and are well summarized in [2]. When the manifold multiplexer is used as the output multiplexer of the satellite transponder, not only the design method but the multipaction aspect should also be taken into consideration. Generally the initial design can be performed by using the equivalent circuit with the simple lumped elements for inverters, but the exact dimensions of the manifold multiplexer cannot be obtained. The three-dimensional full-wave analysis method is used for multipaction analysis and estimating its dimensions. However, such full-wave analysis method may be time consuming and impractical if the filter has a very narrow passband owing to the extreme sensitivity

of the filter performance on dimension<sup>[3],[4]</sup>. Therefore an efficient design method using the accurate equivalent circuit model is required to design a manifold multiplexer and to compute the electrical field at the critical region.

In this paper, we present an efficient multipaction analysis method for the waveguide output multiplexer that consists of the lowpass filters(LPFs) and the manifold multiplexer. While the conventional full-wave analysis method is used for multipaction analysis for LPFs, the equivalent circuit model is employed for channel filters and the manifold to avoid the time consuming and tedious process. Our efficient multipaction analysis method based on the accurate circuit model is applied to the manifold multiplexer for Ka-band satellite transponder and it has been proved to be as accurate as conventional full-wave analysis method.

## II. Output Multiplexer Design

Fig. 1 shows the schematic of a general output multiplexer which consists of LPFs, a test coupler and a manifold multiplexer for Ka band satellite applications.

The LPFs are located at the input of each channel. They are required to provide the high isolation at the reception band as well as to reject the harmonics of the power amplifiers. It should be noted that high power handling capability and high rejection of the harmonics

Manuscript received August 1, 2005 ; revised October 31, 2005. (ID No. 20050801-029J)

<sup>1</sup>Satellite Communications RF Technology Research Team, Electronics and Telecommunications Research Institute(ETRI), Daejeon, Korea.

<sup>2</sup>Department of Electrical Engineering and Computer Science, University of Michigan, USA.

<sup>3</sup>School of Electrical and Electronic Engineering, Chung-Ang University, Seoul, Korea.

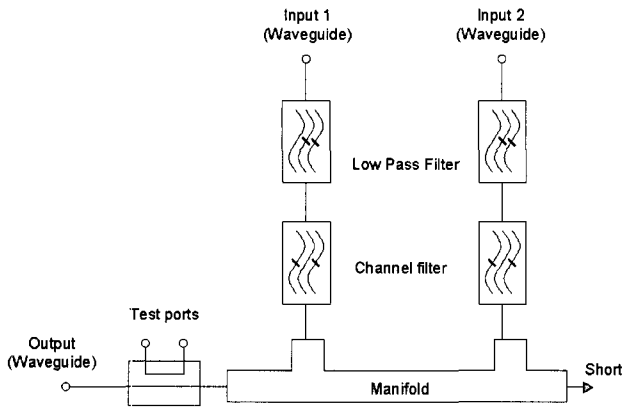


Fig. 1. Block diagram of an output multiplexer.

are contradictory requirements. In the present application, the corrugated LPFs are chosen to meet both the high rejection and high power handling capability requirements. Since the design method of the corrugated filters is well described in many articles<sup>[5],[6]</sup>, this is briefly described in this paper. As shown in Fig. 2, It consists of waveguide transformers and filter section. To suppress the transmission signal at the specific frequency bands such as reception band(30 GHz), 34 GHz and 40 GHz, the dimension of the filter section should be appropriately determined. In the filter section thirteen E-plane waveguide steps are chosen to achieve more than 90 dB isolation at 30 GHz and the waveguide

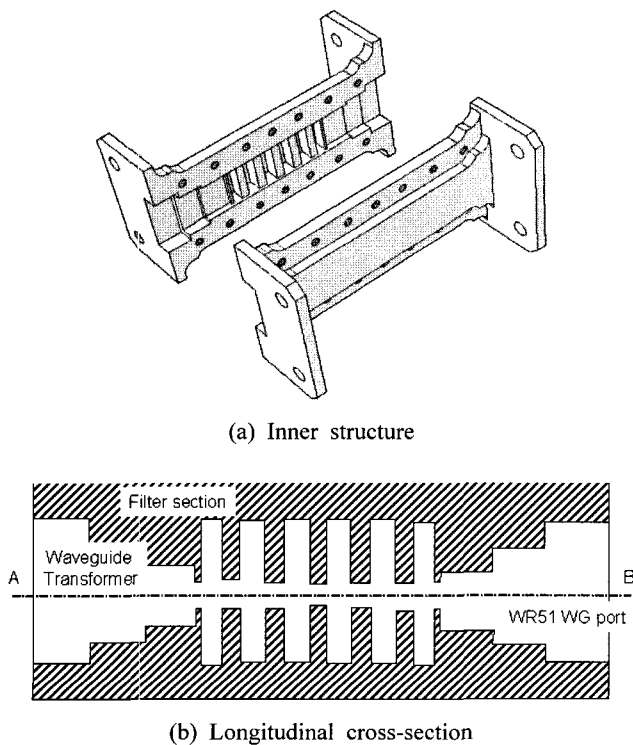


Fig. 2. Configuration of the corrugated lowpass filter.

width of 8.8 mm is used to avoid the TE<sub>20</sub> mode propagation below 34 GHz. The waveguide transformer has one impedance transformer to reduce the insertion loss.

At the design phase, both the electrical parameters and the high power capacity should be considered. Because its minimum gap affects the high power capacity as well as the rejection at the reception band, the appropriate value should be determined. Therefore 1.0 mm of minimum gap is chosen after performing the electrical design and multipaction analysis. We also consider the manufacturing method such as the cutting plane and the diameters of the end-mills to increase the design reliabilities. The interface of the input and the output ports is WR-51. Ansoft HFSS is used to design the corrugated lowpass filter without any tuning elements and the measured results are shown in Fig. 3. The return losses of the design and test result within the passband have more than 28.0 dB and the good agreement is shown in Fig. 3.

A waveguide manifold multiplexer for multiplexing equipment is chosen in this application, since it has both the lowest insertion loss and the minimum mass. It consists of a manifold and channel filters that are directly connected to the T-junction of the manifold. The manifold and each channel filter with a 4-pole elliptic function response are composed of rectangular waveguide line with E-plane T-junction, and dual mode circular waveguide cavities excited on their TE<sub>113</sub> mode, coupling irises and tuning screws. In each cavity, a screw at 45 degrees from the polarization axes couples the dual modes and tuning screws adjust the resonant frequencies. Cross irises ensure couplings between adjacent cavities.

Designing a multi-channel manifold multiplexer is a rather complex task, as the interactions between all the

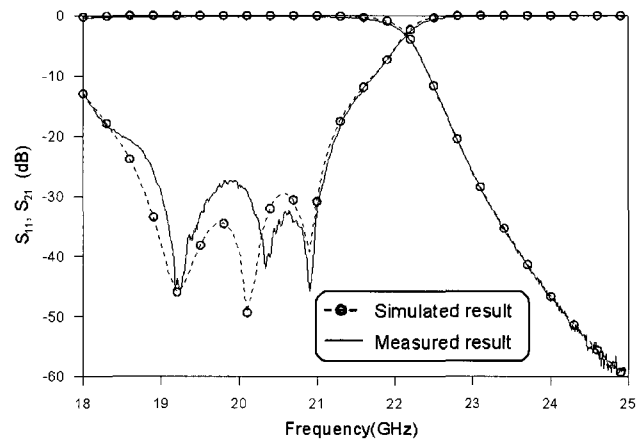


Fig. 3. Measured and simulated results of the lowpass filter.

channels have to be considered. Hence all the parameters (e.g. distance between filters and manifold, couplings, resonant frequencies of the resonators, and so on) have to be optimized to obtain the best performance. Conventionally the simple shunt inductor or the ideal impedance inverter for iris between rectangular waveguide and circular waveguide is used to obtain the initial value during the optimization of manifold multiplexer. In that case, it is difficult to obtain the exact value of manifold dimension such as the distance between the channel filters and the length between the filter and the manifold due to the asymmetric configuration of the irises and thickness of irises. Three-dimensional full-wave method could be possible candidate for optimization. However, setting the manifold multiplexer optimization aside, we can hardly design the narrow-band channel filter only by using full-wave tool such as Ansoft HFSS since the performance of the filter is extremely sensitive to its dimensions.

Therefore, we use an accurate equivalent circuit model for the efficient optimization process for the manifold multiplexer<sup>[7]</sup>. Fig. 4 shows the equivalent circuit of manifold multiplexer with two channel filters and one manifold. This model contains the equivalent circuits for irises, tuning screws, coupling screws, cavity resonators, waveguides and S-parameters of E-plane T-junctions. To obtain the exact waveguide length between the manifold and each channel filter, an asymmetric configuration model for the input and output irises located between a rectangular waveguide and a circular waveguide cavity is used in this circuit model. The equivalent circuit for the irises has the different value of the series inductors due to different types of ports. The coupling iris is of resonant type composed of a shunt inductor and a capacitor. The value of the lumped elements of the iris can be determined from one-pole filter and [7] describes the equation to obtain the value. A symmetric model for inter-cavity iris is adopted because of same ports and the value of lumped elements for equivalent circuit can

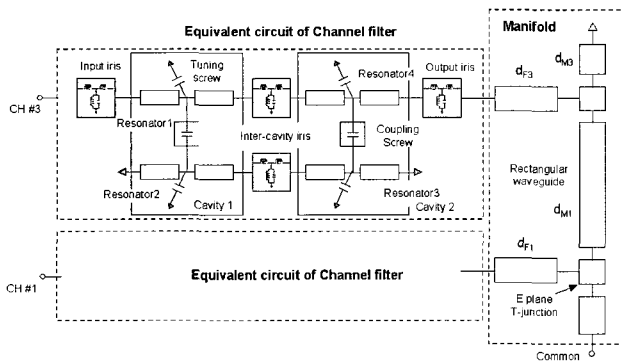


Fig. 4. Equivalent circuit of manifold multiplexer.

be obtained by similar method of input iris. A simple capacitor is used for modeling the tuning and coupling screws. The T-junctions are analytical models derived from a three-dimensional electromagnetic analysis applying the FEM.

The ideal inverters for irises and coupling screws are used to perform the initial design of channel filters. Inverters are substituted by the accurate circuit model which has the same amplitude of  $S_{11}$  between the inverter and the value of the lumped element. The initial values of the waveguide length on the manifold can be determined by well-known theory<sup>[2]</sup>. Finally the design of manifold multiplexer can be performed by an optimization procedure using a circuit simulator such as Advanced Design System (Agilent-ADS) for the computer-aided design. The optimization variables are the length of cavities, the length of input, output and inter-cavity irises and the value of capacitance for coupling and tuning screws.

The fabricated corrugated waveguide LPF which consists of waveguide transformer with double-plane discontinuities and filter section with E-plane discontinuities is split by two halves. They are milled and the diameter of end-mill was considered at the design phase to minimize the difference between design and test result. Any tuning elements are not used.

The output multiplexer is fabricated as shown in Fig. 5. The manifold, LPF and the test coupler of the output multiplexer are constructed out of thin-wall aluminum, which yields the best compromise between electrical, thermal and mechanical performance. All the cavities are manufactured from thin-wall INVAR to minimize the electrical performance degradation in the required temperature range. All the inner surfaces are silver-plated to minimize the losses.

As shown in Fig. 6 for the passband response, the measured results are in very good agreement with the

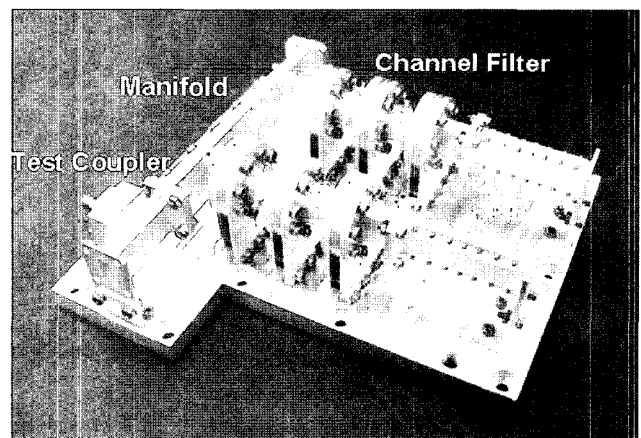


Fig. 5. Fabricated output multiplexer.

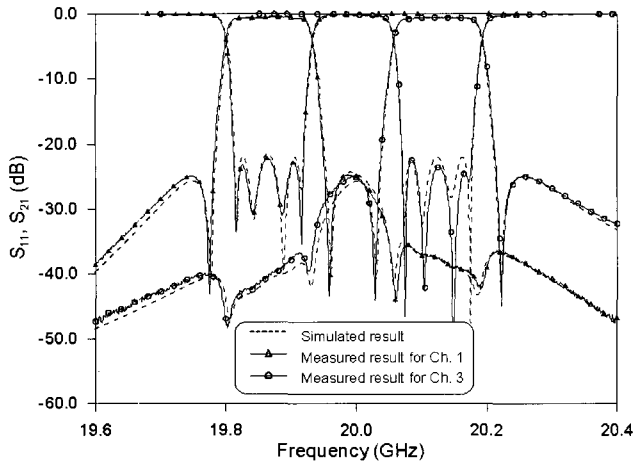


Fig. 6. Design and measurement results of the output multiplexer.

simulated results obtained by using the equivalent circuit proposed in the present study.

### III. Multipaction Analysis

Multipactor is a discharge produced in vacuum when an RF field exists between two surfaces and where the mean free path of the electrons is greater than the gap spacing. Since multipactor causes degradation and failure of waveguide components in satellite RF and microwave payload, multipactor breakdown susceptibility zone must be considered in designing high-power waveguide components. Generally, susceptibility zones given by Woode and Petit<sup>[8]–[10]</sup> are widely adopted in considering multipactor.

Multipaction susceptibility zone is obtained by approximately connecting the envelopes of each breakdown curve drawn by using fitting parameters and computer model equations in [9]. Fig. 7 shows multipaction susceptibility zones for parallel plates of silver plated oxygen free copper. The X-axis of susceptibility zone is the product of the frequency and gap spacing in GHz · mm. This is a constant and allows comparisons to be made between results at different frequencies or gap spacings. The Y-axis is the peak voltage occurring across the gap. Generally, susceptibility zone has one or two slopes and change point between two slopes.

The typical approach to multipaction-free design relies on over-specification and testing. Nowadays, the verification of components using the reliable tool based on electromagnetic field theory is preferred to testing due to the limited output power of amplifier and high test costs for Ka band. In the multipaction analysis, any region where high voltage and critical gaps exist should

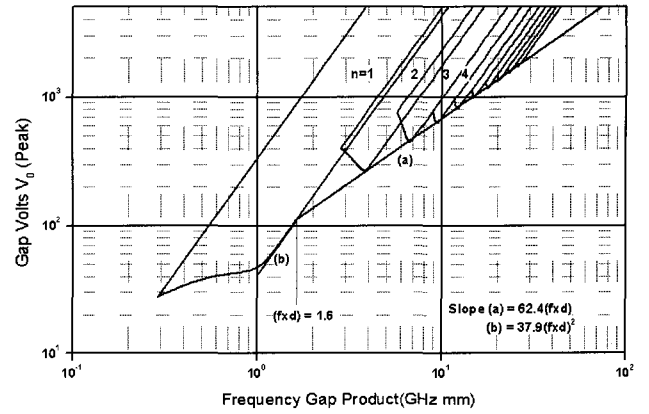


Fig. 7. Multipaction susceptibility zones for parallel plates of silver plated oxygen free copper.

be identified and the peak voltage based on electrical field at the critical region should be computed.

The electrical field in the LPF is obtained from full-wave analysis. Fig. 8 shows the electrical field peak value along the center line of the LPF for 1 watt time-averaged incident power at 20 GHz. This figure shows the fact that the most critical area is located at the center of the LPF. The simulated maximum peak voltage is 33.11 V at the minimum gap. The allowable power related with gap voltage is estimated to be 1,421 W at 20 GHz.

The exact electrical field computation for the multipaction analysis may employ the three-dimensional full-wave analysis. However, as described in the previous section, the full-wave analysis is not practical for the narrow-band dual-mode filters, much less the manifold multiplexer. Therefore, we also use the accurate equivalent circuit model to compute the gap voltages. In the manifold multiplexer, high voltage and low breakdown voltage exist at the center of cavities and at the

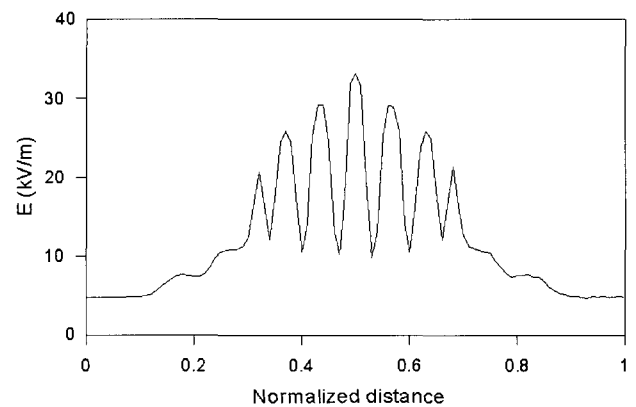


Fig. 8. Electrical field peak value along the center line of the low pass filter(Line AB in Fig. 2).

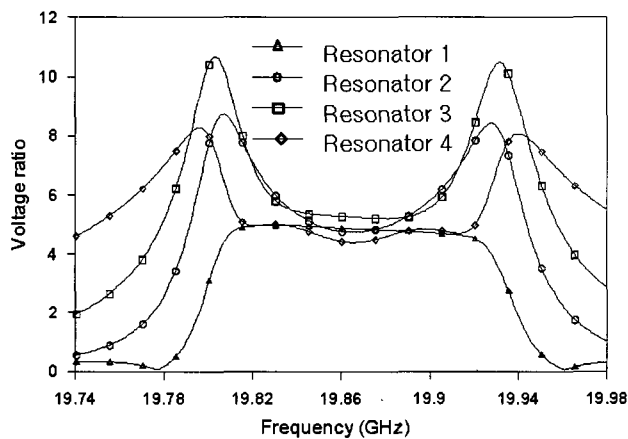
irises, respectively. Therefore the peak voltage should be considered at the center of cavities and irises of channel filters with respect to multipaction. In the multi-carrier operation, the influence from neighbored channels has to be taken into account to compute the maximum electrical field strength at the output irises.

The circuit theory is used to obtain the voltage ratio at the nodes containing the equivalent lumped circuit based on the EM results of the irises and the T-junction. From the voltage ratio and impedance the allowable power at the center of cavities is given by [4],

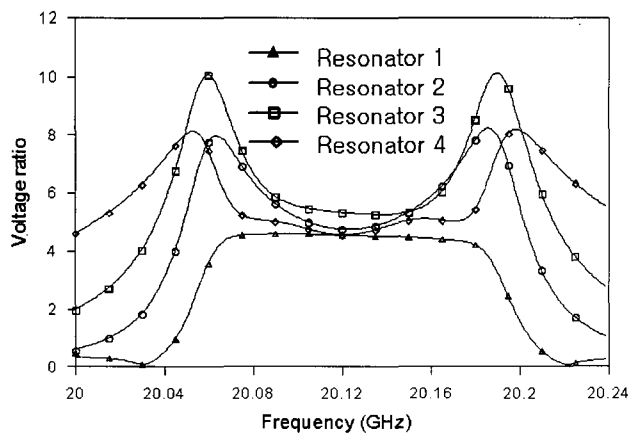
$$P_a = \left( \frac{V_{break}}{\sqrt{2 \cdot Z_{cpv} \cdot V_r}} \right)^2 \tag{1}$$

where  $V_{break}$  is the break-down peak voltage,  $Z_{cpv}$  is the characteristic impedance of the circular waveguide(power-voltage definition) as shown in Table 1 and  $V_r$  is voltage ratio computed by Agilent-ADS at the node. Fig. 8 shows the simulation results of voltage ratio at the center of resonators for each channel filter.

As shown in Fig. 9, the maximum voltage ratio



(a) Channel 1



(b) Channel 3

Fig. 9. The voltage ratio at the center of resonators.

Table 1. Characteristic impedance of circular waveguide.

Frequency(GHz)	$Z_c(\Omega)$
19.80	905.83
19.85	904.86
19.90	903.89
19.95	902.94
20.00	901.99
20.05	901.06
20.10	900.13
20.15	899.22
20.20	898.31

within the passband(19.812~19.919 GHz for channel 1 and 20.071~20.177 GHz for channel 3) occurs at the lowest edge of the passband. From equation (1) and the breakdown voltage in Fig. 7, the allowable powers of 2.92 kW( $V_r$  is 8.83 at 19.812 GHz) for channel 1 and 3.50 kW( $V_r$  is 8.18 at 20.071 GHz) for channel 3 are computed, respectively.

In order to calculate the allowable power at the irises, we should know the voltage at the irises when voltage ratio is one. The allowable power at the iris is given by,

$$P_a = \left( \frac{V_{break}}{V_{iris} \cdot V_r} \right)^2 \tag{2}$$

where  $V_{iris}$  as shown in Table 2 is the peak voltage at the iris.  $V_r$  is the voltage ratio at the node analyzed by ADS. When the voltage ratio is 1,  $V_{iris}$  can be extracted from the simulation results by Ansoft-HFSS and ADS.

Although only single-carrier operation is considered for the allowable power at the center of cavities, multi-carrier operation should be considered at the irises. In multi-carrier operation, voltage ratio should be added in the channel 1 and channel 3 frequency ranges because

Table 2. Voltage at the iris with respect to length of iris.

Length of input iris	$V_{iris}(V)$
6.0 mm	93.4
6.1 mm	92.6
6.2 mm	92.0
6.3 mm	90.6
6.4 mm	89.3
6.5 mm	83.8
6.6 mm	83.0
6.7 mm	82.6
6.8 mm	82.2
6.9 mm	80.7

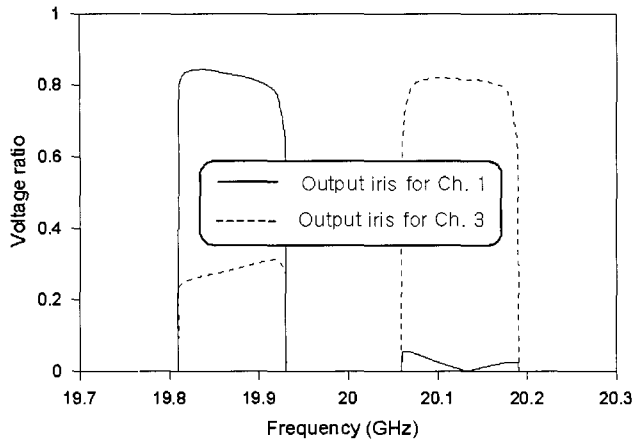


Fig. 10. The voltage ratio at the output irises of channel filters.

a significant contribution of the voltages comes from neighbored channels.

Fig. 10 shows the simulated results of voltage ratio at the output irises of channel filters. The maximum voltage ratio at the output iris of channel 3 filter is 0.32 in the channel 1 frequency range and 0.82 in the channel 1 frequency range, respectively. The allowable power of 811 W is computed at the output irises of filter for channel 3 by (2). The multipaction analysis results for worst case are summarized in Table 3.

The output iris of the channel filter is proved to be the most critical in the manifold multiplexer for high power capability as a computed result. The computed result is compared with the result estimated by mode matching(MM) technique. From this technique, the identification of the most critical point is confirmed as the output iris(manifold side) of channel 3. The maximum electrical field strength at the output iris is computed 580 V/m by MM theory and 576 V/m by this presented theory, respectively. The difference of maximum electrical field at the critical region is confirmed to be less than 2 percent.

#### IV. Conclusion

In this paper, an efficient multipaction analysis method for an output multiplexer which consists of lowpass filters, test coupler and a manifold multiplexer has

been presented. While conventional full-wave analysis method has been used for multipaction analysis for lowpass filters, the effective equivalent circuit model is employed for channel filters and the manifold to avoid the time consuming and tedious process.

Our efficient multipaction analysis method has been applied to the manifold multiplexer for Ka-band satellite transponder and it has been proved to be as accurate as conventional mode matching method.

#### References

- [1] C. Kudsia, R. Cameron, and W. Tang, "Innovations in microwave filters and multiplexing networks for communications satellite systems", *IEEE Trans. on Microwave Theory and Tech.*, vol. 40, no. 6, pp. 1133-1149, Jun. 1992.
- [2] J. Uher, J. Bornemann, and U. Rosenberg, *Waveguide Components for Antenna Feed Systems: Theory and CAD*, Norwood, MA, Artech House, 1993.
- [3] A. Sivasdas, Ming Yu, and R. Cameron, "A simplified analysis for high power microwave bandpass filter structures", *IEEE MTT-S Int. Microwave Symp.*, pp. 1771-1774, 2000.
- [4] M. Ludovich, L. Accatino, G. Zarba, and M. Mongiardo, "CAD of multipactor-free waveguide components for communication satellite", *IEEE MTT-S Int. Microwave Symp.*, Seattle, WA, pp. 2077-2080, 2002.
- [5] L. Young, "Stepped-impedance transformers and filter prototypes", *IEEE Trans. on Microwave Theory and Tech.*, vol. 10, no. 9, pp. 339-359, Sep. 1962.
- [6] R. Levy, "Tables of element values for the distributed low-pass prototype filter", *IEEE Trans. on Microwave Theory and Tech.*, vol. 13, no. 9, pp. 514-536, Sep. 1965.
- [7] M. S. Uhm, J. Lee, J. H. Park, and J. P. Kim, "An efficient optimization design of a manifold multiplexer using an accurate equivalent circuit model of coupling irises of channel filters", *IEEE MTT-S Int. Microwave Symp.*, Long Beach, CA, WEPJ-4, 2005.
- [8] A. D. Woode, J. Petit, "Design data for the control of multipactor discharge in spacecraft microwave and RF systems", *Microwave Journal*, pp. 142-155, Jan. 1992.

Table 3. Multipaction analysis results(Channel filter 1 & 3 with manifold).

Item	Gap (mm)	Freq. (GHz)	$V_{break}(V)$	Gap voltage(V)			$P_a(W)$	Comment
				$V_r$	$V_{iris}$ or $Z_{cpv}$	$V_{gap}$		
Input iris	2.2	19.82	2,721	1.14	< 83.8 V	< 95.5	> 811.8	To manifold
Cavity	16.4	19.82	20,283	< 8.0	< 906 $\Omega$	< 340.5	> 3,548	At the center

[9] A. D. Woode, J. Petit, "Investigation into multipactor breakdown in satellite microwave payload", *ESA Journal*, vol. 14, pp. 467-478, 1990.

[10] *Space Engineering(Multipaction Design and Test)*, ESA Publications Division, ESTEC, Noordwijk, The Netherlands, May 2003.

### Man Seok Uhm



received his B.E. and M.E. degrees in electronic communications engineering from Chungang University, Seoul, Korea in 1987 and 1989, respectively. Since he joined Electronics and Telecommunications Research Institute(ETRI) in 1992, he developed experimental transponder system, antenna, Engineering Qualification model active components and passive components in Satellite Communications Department. His current research interests include the microwave active and passive components, satellite antennas, satellite transponders, and electromagnetic field theories.

### In-Bok Yom



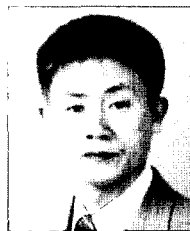
received his B.S. and M.S. degree in electronic communications engineering from Hanyang and Chungnam National University, South Korea in 1990 and 2004, respectively. Since he joined ETRI in 1990, he developed experimental transponder system, engineering qualification model active components and passive components in Satellite Communications Department. He is also currently the chief of satellite communications RF technique team in ETRI. His current research interests include the microwave active and passive components, satellite transponders, and electromagnetic field theories.

### Juseop Lee



is currently a graduate student in Electrical Engineering and Computer Science at the University of Michigan, Ann Arbor, MI, where he is working toward his Ph.D. degree. He received his B.S. and M.S. degree in radio science and engineering from Korea University, Seoul, South Korea, in 1997 and 1999, respectively. He worked as a research engineer at LG Electronics(formerly LG Information and Communications), South Korea, and ETRI(Electronics and Telecommunications Research Institute), South Korea, from 1999 to 2001 and from 2001 to 2005, respectively. He was involved in the project for performance and reliability analysis of RF components for CDMA systems and development of passive RF equipment for Ku- and Ka-band communications satellites. He returned to school in September 2005. His research interests include the RF and microwave components, satellite transponders, and electromagnetic field theories.

### Jeong-Phill Kim



received his B.S. degree in electronic engineering from Seoul National University, Seoul, Korea, in 1988, the M.S. and Ph.D. degrees in electronic engineering from Pohang University of Science and Technology, Pohang, Korea, in 1990 and 1998, respectively. From 1990 to 2001, he was a research engineer in the R&D Center at LG Innotek, Korea, where he was involved with the design of antennas, transmitters, and receivers for various radar systems. Since 2001, he has been a faculty member with the school of electrical and electronic engineering, Chung-Ang University, Seoul, Korea. His current research interests include the design of antennas, RF and microwave components, on-chip tunable filter, RFID system applications, and various communication applications of true random signals.